PHYSICAL REVIEW B **74**, 184417 (2006)

Phase relations in the Li_2O-V_2O_3-V_2O_5 system at 700 °C: Correlations with magnetic-defect concentration in heavy fermion LiV_2O_4

S. Das, X. Ma,* X. Zong, A. Niazi, and D. C. Johnston
Ames Laboratory and Department of Physics and Astronomy, Iowa State University, Ames, Iowa 50011, USA

(Received 31 July 2006; revised manuscript received 31 August 2006; published 16 November 2006)

The phase relations in the Li_2O-V_2O_3-V_2O_5 ternary system at 700 °C for compositions in equilibrium with LiV_2O_4 are reported. This study clarified the synthesis conditions under which low and high magnetic defect concentrations can be obtained within the spinel structure of LiV_2O_4. We confirmed that the LiV_2O_4 phase can be obtained containing low (0.006 mol %) to high (0.83 mol %) magnetic defect concentrations n_{defect} and with consistently high magnetic defect spin S values between 3 and 6.5. The high n_{defect} values were obtained in the LiV_2O_4 phase in equilibrium with V_2O_3, Li_3VO_4, or $LiVO_2$ and the low values in the LiV_2O_4 phase in equilibrium with V_3O_5. A model is suggested to explain this correlation.

DOI: 10.1103/PhysRevB.74.184417 PACS number(s): 75.20.Hr, 81.30.Dz, 71.27.+a

I. INTRODUCTION

Heavy fermion (HF) behavior has mostly been seen in f-electron metals. Such compounds are called heavy fermions because in these materials the current carriers behave as if they have a large mass ($\sim 10^2 - 10^3$ times the free electron mass). LiV_2O_4, first synthesized by Reuter and Jaskowsky,[1] is one of the few d-electron compounds to show HF behavior at low temperatures.[2,3] LiV_2O_4 has the face-centered-cubic spinel structure with the space group $Fd\bar{3}m$. The V atoms are coordinated by six O atoms in a slightly distorted octahedron. The Li atoms are coordinated with four O atoms in a tetrahedron. The Li atoms are located in the gaps between chains of the VO_6 edge-sharing octahedra. From NMR measurements done on LiV_2O_4 samples it has been found that for magnetically pure samples the ^{7}Li nuclear spin-lattice relaxation rate $1/T_1$ is proportional to temperature T at low temperatures (the Korringa law) which is typical for Fermi liquids.[2,4,5] However, for samples which contain magnetic defects within the spinel structure, the relaxation rate has a peak at ∼1 K and also shows other signatures which do not agree with the behavior of Fermi liquids.[6] The occurrence of magnetic defects is easily seen as a low-T Curie-like upturn in the magnetic susceptibility rather than becoming nearly independent of T below ∼10 K as observed for the intrinsic behavior.[7] The mechanism for the formation of the magnetic defects is not known yet.

Previously, polycrystalline samples of LiV_2O_4 had been prepared from the starting materials Li_2CO_3, V_2O_3, and V_2O_5 at 700 °C. Typically, the samples contain a concentration of magnetic defects n_{defect} within the structure of the spinel phase, ranging from $\lesssim 0.01$ to 0.7 mol %.[7] Magnetization M versus applied magnetic field H measurements at low T were carried out to estimate n_{defect} and the defect spin S_{defect}. Low concentrations of defects were found in samples of LiV_2O_4 containing small amounts of V_3O_5 impurity phase while high defect concentrations were found in samples containing V_2O_3 impurity phase.[7] Though the reason behind this correlation is not yet known, these results pointed toward a controllable way to vary the magnetic defect concentration within the spinel structure. However, it was not clear that the above-noted V_2O_3 and V_3O_5 impurity phases were in equilibrium with the LiV_2O_4 spinel phase at 700 °C. In addition, it was unknown (in Ref. 7) how the magnetic defect concentration in the spinel phase LiV_2O_4 varied if other impurity phases were present. To help resolve these questions, we report here the phase relations in the Li_2O-V_2O_3-V_2O_5 system at 700 °C, in the vicinity of the composition LiV_2O_4, and report the magnetic properties of a selection of such compositions.

There have been some studies of the Li_2O-V_2O_5 system which revealed the existence of three phases in the system, namely $LiVO_3$, Li_3VO_4, and LiV_3O_8. Reisman *et al.*[8] reported the existence of the congruently melting phases $LiVO_3$ (reported as $Li_2O \cdot V_2O_5$) and Li_3VO_4 (reported as $3Li_2O \cdot V_2O_5$) with melting points 616 °C and 1152 °C, respectively. LiV_3O_8 has been reported to be both congruently melting and incongruently melting.[8–10] Manthiram *et al.*[11] reported that $Li_{1-x}VO_2$ is single phase in the compositional range $0 \leqslant x \leqslant 0.3$ at 650 °C. LiV_2O_4 was reported to exist in equilibrium with the compounds VO_2 and $Li_{1-x}VO_2$ from room temperature to 1000 °C by Goodenough *et al.*[12] The lithium vanadium oxide system $Li_xV_2O_5$, also known as the lithium vanadium bronze phase, was reported to exist in a number of single-phase regions for $0 < x < 1$ and temperature $T < 500$ °C (Ref. 13).

The V_2O_3-V_2O_5 binary system has been extensively studied and a large number of phases have been reported. Hoschek and Klemm[14] first studied the system and suggested the presence of the phase V_2O_3, the β-phase ($VO_{1.65}$-$VO_{1.80}$), the α-phase ($VO_{1.80}$-VO_2), and the α'-phase ($VO_{2.09}$-$VO_{2.23}$). Andersson[15] reported phases with the general formula V_nO_{2n-1} with $3 \leqslant n < 9$. Additional phases reported in this system are V_9O_{17} and $V_{10}O_{19}$ (Ref. 16). The phases with the general formula V_nO_{2n-1} with $3 \leqslant n \leqslant 9$ are called the Magnéli phases.[17] The triclinic structure of the Magnéli phases have been reported.[15,16,18,19] The other V-O phases existing between VO_2 and V_2O_5 are V_6O_{13} (Refs. 15 and 20), V_4O_9 (Ref. 21), and V_3O_7 (Refs. 22 and 23). Combined with the work by Kachi and Roy,[24] Kosuge[23] proposed a phase diagram of the V_2O_3-V_2O_5 system in the temperature-composition plane extending from room temperature to 1200 °C showing high melting points (>1200 °C) for V-O phases existing between V_2O_3 and

VO_2, low melting points ($\lesssim$700 °C) for V-O phases existing between VO_2 and V_2O_5 and also the homogeneity ranges of all the phases existing between V_2O_3 and V_2O_5.

II. EXPERIMENTAL DETAILS

Our samples were prepared by conventional solid state reaction as described by Kondo *et al.*[7] The starting materials were Li_2CO_3 (99.995%, Alfa Aesar), V_2O_5 (99.995%, M V Laboratories Inc.), and V_2O_3 (99.999%, M V Laboratories Inc.). The samples were made in two stages. First a $(Li_2O)_x(V_2O_5)_y$ precursor was made by thoroughly mixing appropriate amounts of Li_2CO_3 and V_2O_5, pressing into a pellet and then heating in a tube furnace under oxygen flow at 525 °C until the expected weight loss occurred due to the loss of CO_2 from Li_2CO_3. The precursor pellet was then crushed and the appropriate amount of V_2O_3 was added and mixed thoroughly inside a helium-filled glove box. The precursor-V_2O_3 mixture was then again pressed into a pellet, wrapped in a platinum foil, sealed in a quartz tube under vacuum and then heated at 700 °C for about ten days. The samples were taken out of the furnace and air-cooled to room temperature. The different phases present in the samples were identified from x-ray diffraction patterns at room temperature obtained using a Rikagu Geigerflex diffractometer with a curved graphite crystal monochromator. The diffraction patterns were matched with known phases from the JCPDS (Ref. 25) database using the JADE 7 program.[26] The samples were repeatedly ground and heated until the x-ray patterns did not show any change to ensure that the samples were in thermal equilibrium at 700 °C. The magnetization M_{obs} measurements were done on the samples using a quantum design superconducting quantum interference device (SQUID) magnetometer over the temperature T range 1.8–350 K and applied magnetic field H range 0.001 T–5.5 T.

III. RESULTS AND ANALYSIS

A. Phase relations at 700 °C

The phase relations for phases in equilibrium with LiV_2O_4 at 700 °C are shown in Fig. 1. The black triangles represent the crystalline phases which exist singly in equilibrium at 700 °C. The solid dots represent the compositions of our samples from which the phase relations were determined. The solid straight lines connecting the phases are the tie lines. From a large number of samples synthesized at the nominal stoichiometric composition LiV_2O_4, it has been found that LiV_2O_4 is a "line compound," i.e., this compound has an extremely small ($\lesssim$1 at. %) homogeneity range. This situation is very different from the large homogeneity range $0 \leqslant x \leqslant 1/3$ in the similiar spinel phase $Li[Li_xTi_{2-x}]O_4$.[27] According to the study of $Li_{1-x}VO_2$ by Goodenough *et al.*[12] mentioned above, there is a tie line between LiV_2O_4 and $LiVO_2$ at 700 °C, consistent with our results. However, our results conflict with their finding of a tie line between LiV_2O_4 and VO_2. In particular, the observed tie line in Fig. 1 between V_4O_7 and Li_3VO_4 precludes a tie line between LiV_2O_4 and VO_2 because the latter would have to cross the former which is not allowed.

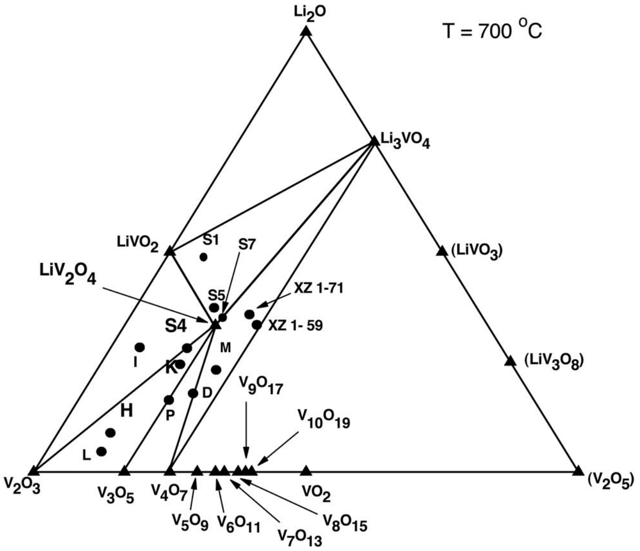

FIG. 1. Phase relations in the Li_2O-V_2O_3-V_2O_5 system at 700 °C for phases in equilibrium with the LiV_2O_4 spinel phase. The triangles represent the crystalline phases which exist singly in equilibrium at 700 °C. The dots represent the compositions of our samples from which the phase relations were determined. The solid straight lines connecting the phases are the tie lines. The compounds in parentheses melt below 700 °C.

B. Magnetic measurements

1. Magnetic susceptibility measurements

Here we present the magnetic susceptibility χ versus temperature T for some of our samples of LiV_2O_4 containing small amounts ($\lesssim$2 wt %) of impurity phases. Based on the x-ray diffraction patterns, the impurity phases present in the samples are V_2O_3 in sample 5A, V_3O_5 in sample 8, $LiVO_2$ in sample 5B, and Li_3VO_4 in sample S7 as shown in Table I. Sample 6B was the crystallographically purest sample synthesized and the x-ray diffraction pattern did not reveal any impurity phases. Figures 2 and 3 show expanded x-ray diffraction patterns of these samples.

The observed magnetic susceptibility χ_{obs} versus T plots from T=1.8 K to 350 K at magnetic field H=1 T for the five samples are shown in Fig. 4 where $\chi_{obs} \equiv M_{obs}/H$. It can be clearly seen that the dependence of χ_{obs} on T for the five samples is similar Curie-Weiss like for T>50 K. However, for T<50 K the dependence is strikingly different. Sample 8 containing V_3O_5 impurity phase shows a broad peak at $T \approx 20$ K, which is characteristic of the intrinsic behavior of magnetically pure LiV_2O_4.[7] Sample 6B which is crystallographically pure also shows a broad peak but it is masked by a Curie-like upturn at T<10 K. For sample 5A containing V_2O_3, S7 containing Li_3VO_4, and 5B containing $LiVO_2$ as impurity phases, the broad peak is totally masked by Curie contributions.

To interpret the origin of the Curie-like low-T contributions to $\chi(T)$ of these samples, it is important to consider the

TABLE I. Results of the analyses of the $M_{\rm obs}(H,T)$. The error in the last digit of a parameter is given in parentheses.

Sample No.	Impurity	χ (cm^3/mol)	$n_{\rm defect}$ (mol %)	$S_{\rm defect}$	$\theta_{\rm defect}$ (K)	$n_{\rm defect}S_{\rm defect}$ (mol %)
5A	V_2O_3	0.0123(1)	0.77(3)	4.0(1)	−0.70(13)	3.08(13)
S7	Li_3VO_4	0.0115(1)	0.67(2)	3.7(1)	−0.59(9)	2.52(8)
8	V_3O_5	0.0098(1)	0.0067(28)	6.3(27)	−1.0(10)	0.04(18)
5B	$LiVO_2$	0.0127(2)	0.83(3)	3.9(1)	−0.65(12)	3.29(13)
6B	no impurity	0.0104(1)	0.21(1)	3.5(2)	−0.75(13)	0.73(4)

potential contributions of the impurity phases to this term. V_3O_5 orders antiferromagnetically with its susceptibility showing a very broad maximum between $T=120$ K and 130 K (Refs. 28 and 29) which is much higher than its Néel temperature $T_N=75.5$K measured by Griffing.[30] The susceptibility for $T<T_N$ decreases with decreasing T, has a value $<2\times10^{-5}$ cm^3/mol at the lowest temperatures, and shows no evidence for a Curie-like term. V_2O_3 has a Curie-Weiss-like behavior for $T>170$ K where it is also metallic. Below 170 K it orders antiferromagnetically at a metal to insulator transition and the susceptibility remains constant at about 5×10^{-4} cm^3/mol down to $T\sim80$ K. For $T<80$ K, the susceptibility decreases with decreasing T with no sign of a Curie-like upturn.[29,31] The susceptibility of $V_{2-y}O_3$ shows a peak at low T ($\sim$10 K) as it undergoes antiferromagnetic ordering at around 10 K with no evidence for a Curie-like term at lower T.[29] Li_3VO_4 is nonmagnetic since the vanadium atom is in the +5 oxidation state. The only impurity phase exhibiting a low-temperature Curie-like contribution to its susceptibility is $Li_{1-x}VO_2$, which shows a Curie-like upturn at $T<50$ K due to Li deficiency of about 5%.[32,33] However, the amounts of impurity phases in our LiV_2O_4 samples are small (<2 wt %). Assuming that $x=0.05$ in $Li_{1-x}VO_2$ impurity phase,[32] where each Li vacancy induces a V^{+4} ($S=1/2$) defect in that phase, one obtains a Curie constant of $\simeq4\times10^{-4}$ cm^3 K/mol, which is far smaller than observed ($\sim$0.1 cm^3 K/mol) in our sample 5B having a $Li_{1-x}VO_2$ impurity phase. Thus we can conclude that the Curie-like upturn in the susceptibility of nearly single-phase LiV_2O_4 arises from magnetic defects within the spinel structure of this compound and not from impurity phases, which confirms the previous conclusion of Ref. 7.

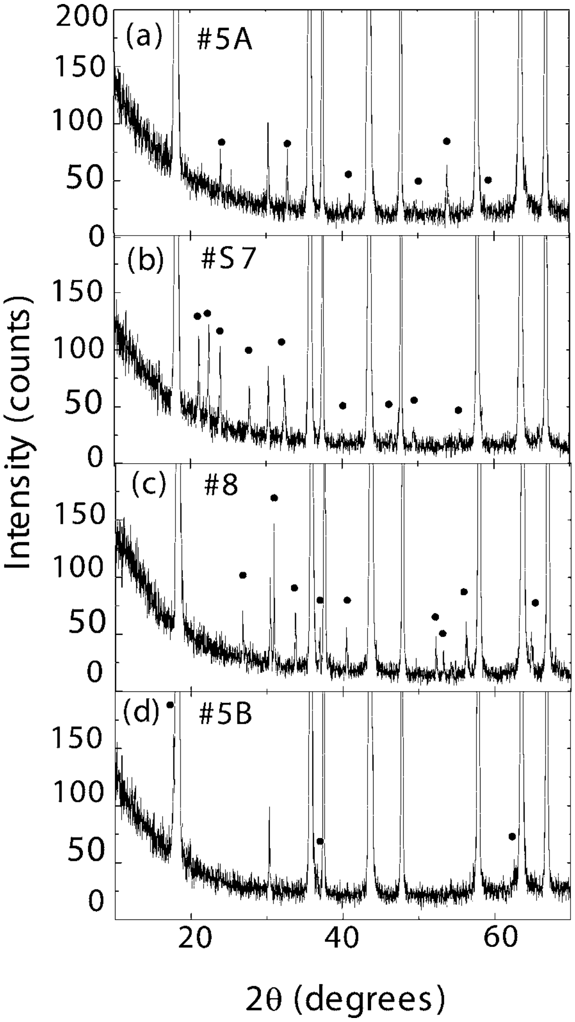

FIG. 2. Expanded x-ray diffraction patterns of samples with compositions near LiV_2O_4. The impurity phase peaks are marked by solid circles. (a) Sample 5A has V_2O_3 impurity phase. (b) Sample S7 has Li_3VO_4 impurity phase. (c) Sample 8 has V_3O_5 impurity phase. (d) Sample 5B has $LiVO_2$ impurity phase.

2. Isothermal magnetization measurements

The observed magnetization $M_{\rm obs}$ versus applied magnetic field H isothermal measurements were done at different tem-

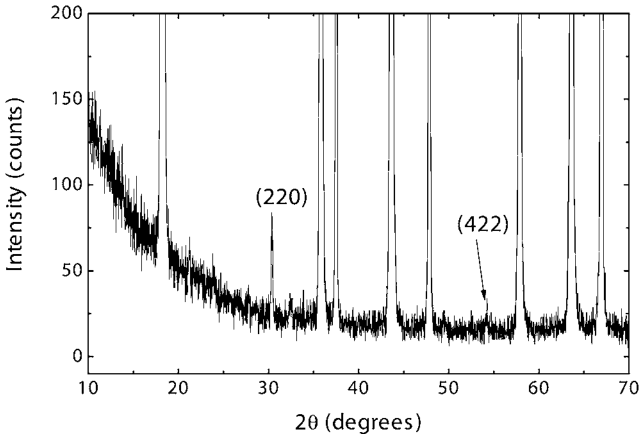

FIG. 3. Expanded x-ray diffraction pattern of the LiV_2O_4 sample 6B. The two indexed peaks are of the LiV_2O_4 spinel phase. There are no observable impurity phases present.

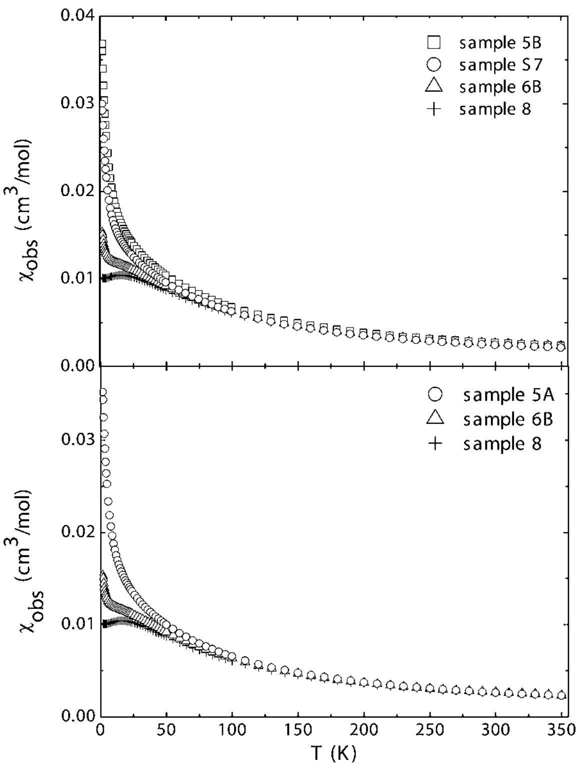

FIG. 4. Observed magnetic susceptibility χ_{obs} versus temperature T at $H=1$ T for several samples in Table I that are nearly single-phase LiV_2O_4.

peratures between 1.8 and 350 K with H varying from 0.001 to 5.5 T. However, to find n_{defect} only the low T (1.8, 2.5, 3, and 5 K) isotherms were used. The M_{obs} versus H curves for different samples at 1.8 K are shown in Fig. 5. The samples showing a Curie-like upturn in the susceptibility show a negative curvature in their M_{obs} versus H curves, whereas the samples having a very small Curie-like upturn in the susceptibility show a hardly observable curvature. This correlation shows that the Curie contribution to the susceptibility is due to field saturable (paramagnetic) defects. The values of the defect concentrations and the values of the defect spins for different samples were determined according to the analysis done by Kondo *et al.*[7] The observed molar magnetization M_{obs} isotherms at low temperatures ($T \lesssim 5$ K) for each sample were simultaneously fitted by

$$M_{obs} = \chi H + n_{defect} N_A g_{defect} \mu_B S_{defect} B_S(x), \qquad (1)$$

where n_{defect} is the concentration of the magnetic defects, N_A Avogadro's number, g_{defect} the g factor of the defect spins which was fixed to two (the detailed reasoning behind this is given in Ref. 7), S_{defect} the spin of the defects, $B_S(x)$ the Brillouin function, and χ the intrinsic susceptibility of the LiV_2O_4 spinel phase. The argument of the Brillouin function $B_S(x)$ is $x = g_{defect}\mu_B S_{defect} H / [k_B(T-\theta_{defect})]$ where θ_{defect} is the Weiss temperature. The four fitting parameters χ, n_{defect}, S_{defect}, and θ_{defect} for each sample are listed in Table I. Since the parameters n_{defect} and S_{defect} are strongly correlated in the fits, the products of these are also listed in Table I.

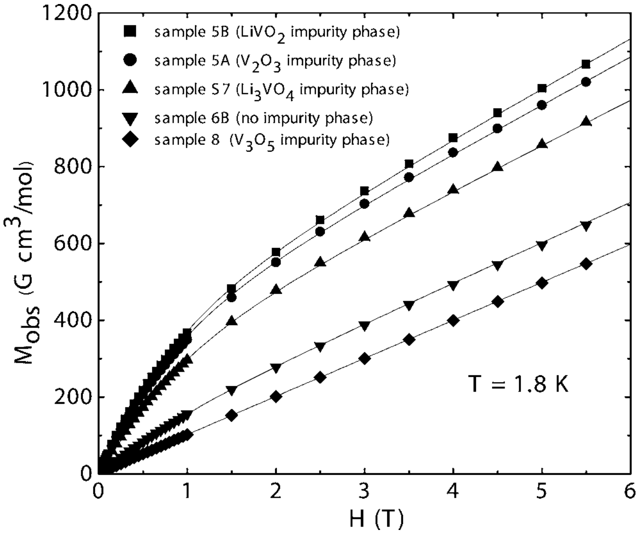

FIG. 5. M_{obs} versus H isotherms of four samples at 1.8 K. The curves passing through the data points are fits by Eq. (1) with the values of the parameters given in Table I.

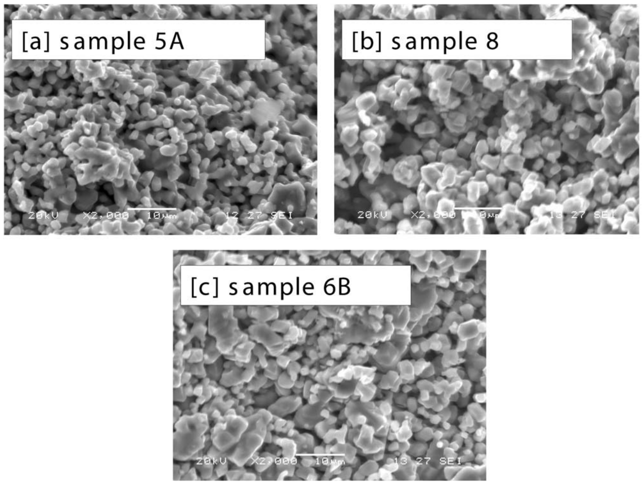

FIG. 6. SEM pictures of our LiV_2O_4 powder samples. No evident correlation between the grain sizes and the defect concentrations was found. The bars at the bottom of each picture are 10 μm long. The grain sizes are in the range 1 to 10 μm.

The grain sizes of our samples were studied using a scanning electron microscope (SEM). The SEM pictures of some of our samples are shown in Fig. 6. As seen from the figure, the grain sizes are 1–10 μm, and from Table I there is no evident correlation between the sample grain sizes and the magnetic defect concentrations.

IV. SUGGESTED MODEL

The reason behind the correlation between the presence of the Li-V-O and V-O phases and the variation of the magnetic defect concentration in LiV_2O_4 is not known yet. We speculate that this is due to the formation of vacancies and/or interstitials in the spinel structure due to the variation of the sample composition from the ideal stoichiometry. A possible model is shown in Fig. 7. The black triangle is stoichiometric LiV_2O_4 while the circular region is a small ($\lesssim 1$ at. %) ho-

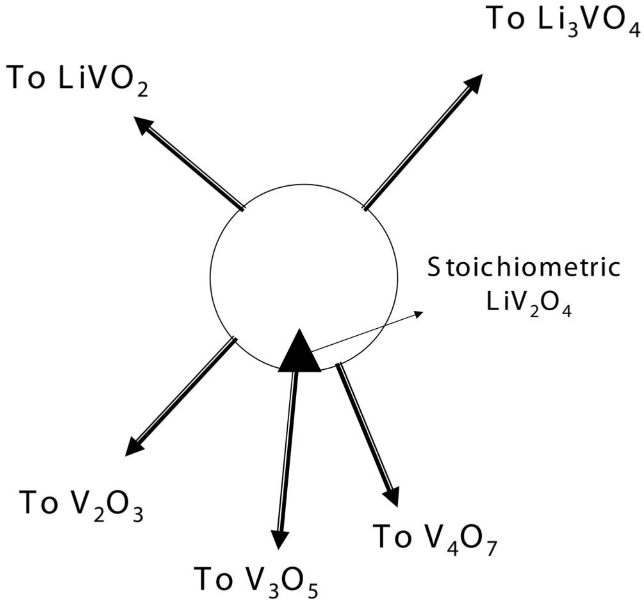

FIG. 7. Suggested model for the mechanism of the crystal and magnetic defect formation in LiV_2O_4. The figure shows an enlarged region around LiV_2O_4 in the phase relation picture (Fig. 1) where the circle represents a possible small homogeneity range of the spinel phase and the filled triangle is stoichiometric LiV_2O_4.

mogeneity range of LiV_2O_4. Based on this model, the LiV_2O_4 phase in the samples having a V_3O_5 impurity phase are very close to the ideal stoichiometric LiV_2O_4, the magnetic susceptibility is the intrinsic susceptibility for the ideal stoichiometric spinel phase and the magnetic defect concentration is very small. The composition of the spinel phase in samples having V_2O_3, Li_3VO_4, or $LiVO_2$ as impurity phases deviates from the ideal stoichiometry as can be seen in the figure. This variation from the ideal stoichiometry would cause the above vacancies and/or interstitial defects to form which in turn cause the formation of paramagnetic defects. The samples having chemical composition different from the black solid triangle (i.e., the ideal stoichiometric composition) but within the circular region will be by definition single phase LiV_2O_4 but not having the ideal stoichiometry. Thus some samples of LiV_2O_4 will have magnetic defects even if there are no impurity phases in them which might be the case for our sample 6B and also samples 3 and 7 studied by Kondo *et al.*,[7] where some samples were essentially impurity free but still had a strong Curie contribution in their susceptibility.

V. CONCLUSION

In this paper we have reported the phase relations in the Li_2O-V_2O_3-V_2O_5 system at 700 °C for compositions in equilibrium with LiV_2O_4. This study helped us to determine the synthesis conditions under which polycrystalline samples of LiV_2O_4 could be prepared with variable magnetic defect concentrations ranging from $n_{\text{defect}}=0.006$ to 0.83 mol %. High magnetic defect concentrations were found in samples containing V_2O_3, Li_3VO_4, or $LiVO_2$ impurity phases while the samples containing a V_3O_5 impurity phase had low defect concentration. We suggested a possible model which might explain this correlation. Our work shows how to systematically and controllably synthesize LiV_2O_4 samples with variable magnetic defect concentrations within the spinel structure. The results should be helpful to other researchers synthesizing samples for study of the physical properties of this system.

ACKNOWLEDGMENTS

Ames Laboratory is operated for the U. S. Department of Energy by Iowa State University under Contract No. W-7405-Eng-82. This work was supported by the Director for Energy Research, Office of Basic Energy Sciences.

---

*Present address: Chemical Physics Program, Institute for Physical Science and Technology, University of Maryland, College Park, MD 20742, USA.

[1] B. Reuter and J. Jaskowsky, Angew. Chem. **72**, 209 (1960).

[2] S. Kondo, D. C. Johnston, C. A. Swenson, F. Borsa, A. V. Mahajan, L. L. Miller, T. Gu, A. I. Goldman, M. B. Maple, D. A. Gajewski, E. J. Freeman, N. R. Dilley, R. P. Dickey, J. Merrin, K. Kojima, G. M. Luke, Y. J. Uemura, O. Chmaissem, and J. D. Jorgensen, Phys. Rev. Lett. **78**, 3729 (1997).

[3] D. C. Johnston, Physica B **281–282**, 21 (2000).

[4] A. V. Mahajan, R. Sala, E. Lee, F. Borsa, S. Kondo, and D. C. Johnston, Phys. Rev. B **57**, 8890 (1998).

[5] K. Fujiwara, K. Miyoshi, J. Takeuchi, Y. Shimaoka, and T. Kobayashi, J. Phys.: Condens. Matter **16**, S615 (2004).

[6] D. C. Johnston, S. H. Baek, X. Zong, F. Borsa, J. Schmalian, and S. Kondo, Phys. Rev. Lett. **95**, 176408 (2005).

[7] S. Kondo, D. C. Johnston, and L. L. Miller, Phys. Rev. B **59**, 2609 (1999).

[8] A. Reisman and J. Mineo, J. Phys. Chem. **66**, 1181 (1962).

[9] R. Kohmüller and J. Martin, Bull. Soc. Chim. Fr. **4**, 748 (1961).

[10] D. G. Wickham, J. Inorg. Nucl. Chem. **27**, 1939 (1965).

[11] A. Manthiram and J. B. Goodenough, Can. J. Phys. **65**, 1309 (1986).

[12] J. B. Goodenough, G. Dutta, and A. Manthiram, Phys. Rev. B **43**, 10170 (1991).

[13] D. W. Murphy, P. A. Christian, F. J. DiSalvo, and J. V. Waszczak, Inorg. Chem. **18**, 2800 (1979).

[14] Cited in Ref. 23 as E. Hoschek and W. Klemm, Z. Anorg Z. Anorg. Allg. Chem. **242**, 63 (1939).

[15] G. Andersson, Acta Chem. Scand. (1947-1973) **8**, 1599 (1954).

[16] H. Kuwamoto, N. Otsuka, and H. Sato, J. Solid State Chem. **36**, 133 (1981).

[17] A. Magnéli, Acta Chem. Scand. (1947-1973) **2**, 501 (1948).

[18] S. Andersson and L. Jahnberg, Ark. Kemi **21**, 413 (1963).

[19] H. Horiuchi, N. Morimoto, and M. Tokonami, J. Solid State Chem. **17**, 407 (1976).

[20] F. Aebi, Helv. Chim. Acta **31**, 8 (1948).
[21] K. A. Wilhelmi and K. Waltersson, Acta Chem. Scand. (1947-1973) **24**, 9 (1970).
[22] J. Tudo and G. Tridot, Compt. Rend. **261**, 2911 (1965).
[23] K. Kosuge, J. Phys. Chem. Solids **28**, 1613 (1966).
[24] Cited in Ref. 23 as S. Kachi and R. Roy, Second Quarterly Report on Crystal Chemistry Studies, Pennsylvania State University, 4 December (1965).
[25] International Centre for Crystal Data, 12 Campus Boulevard, Newtown Square, Pennsylvania 19073-3273 U.S.A. (www.icdd.com).
[26] Materials Data Inc., 1224 Concannon Blvd., Livermore, California 94550 U.S.A. (www.materialsdata. com).
[27] D. C. Johnston, J. Low Temp. Phys. **25**, 145 (1976).
[28] S. Nagata, P. H. Keesom, and S. P. Faile, Phys. Rev. B **20**, 2886 (1979).
[29] Y. Ueda, J. Kikuchi, and H. Yasuoka, J. Magn. Magn. Mater. **147**, 195 (1995).
[30] Cited in Ref. 28 as B. F. Griffings (private communication).
[31] J. Kikuchi, N. Wada, K. Nara, and K. Motoya, J. Phys. Chem. Solids **63**, 969 (2002).
[32] W. Tian, M. F. Chisholm, P. G. Khalifah, R. Jin, B. C. Sales, S. E. Nagler, and D. Mandrus, Mater. Res. Bull. **39**, 1319 (2004).
[33] M. Onoda, T. Naka, and H. Nagasawa, J. Phys. Soc. Jpn. **60**, 2550 (1991).